Subsurface damage distribution characterization of ground surfaces using Abbott–Firestone curves

Raynald Laheurte, Philippe Darnis, Nathalie Darbois, Olivier Cahuc, Jérôme Neauport

Subsurface damage distribution characterization of ground surfaces using Abbott–Firestone curves

Raynald Laheurte,[1,2,3,*] Philippe Darnis,[1,2,3] Nathalie Darbois,[4] Olivier Cahuc,[1,2,3] and Jérôme Neauport[4]

[1]*Univ. Bordeaux, I2M, UMR 5295, F-33400 Talence, France*
[2]*CNRS, I2M, UMR 5295, F-33400 Talence, France*
[3]*Arts et Metiers ParisTech, I2M, UMR 5295, F-33400 Talence, France*
[4]*Commissariat à l'énergie atomique, Centre d'études scientifiques et techniques d'Aquitaine, BP 2, 33114 Le Barp, France*
raynald.laheurte@u-bordeaux1.fr

Abstract: Measurement of subsurface damage (SSD) induced by grinding process is of major interest in the development of high laser damage fused silica optical components manufacturing processes. Most SSD measurements methods give only access to the peak to peak value. We herein report on the benefit of using Abbott–Firestone curves to get an insight of the SSD distribution inside the optical material. We evidence on various diamond wheel ground fused silica substrates that such an approach is complementary to a classical SSD peak to peak measurement and bring useful information to optimize a grinding process.

OCIS codes: (140.3330) Lasers and laser optics: laser damage; (220.1920) Optical design and fabrication: diamond machining.

References and links

1. M. D. Feit and A. M. Rubenchik, "Influence of subsurface cracks on laser induced surface damage," Proc. SPIE **5273**, 264–272 (2004).
2. M. A. Josse, H. Bercegol, R. Courchinoux, T. Donval, L. Lamaignère, B. Pussacq, and J. L. Rullier, "Study of the evolution of mechanical defects on silica samples under laser irradiation at 355 nm," Proc. SPIE **6403**, 64030E, 64030E-7 (2006).
3. J. Lambropoulos, "Micromechanics of material-removal mechanisms from brittle surfaces," LLE Review **74**, 131–138 (1998).
4. Y. Zhou, D. Funkenbusch, D. J. Quesnel, D. Golini, and A. Lindquist, "Effect of etching and imaging mode on the measurement of subsurface damage in microground optical glasses," J. Am. Ceram. Soc. **77**(12), 3277–3280 (1994).
5. J. A. Randi, J. C. Lambropoulos, and S. D. Jacobs, "Subsurface damage in some single crystalline optical materials," Appl. Opt. **44**(12), 2241–2249 (2005).
6. T. Suratwala, L. Wong, P. Miller, M. D. Feit, J. Menapace, R. Steele, P. Davis, and D. Walmer, "Sub-surface mechanical damage distributions during grinding of fused silica," J. Non-Cryst. Solids **352**(52-54), 5601–5617 (2006).
7. F. W. Preston, "The structure of abraded glass surfaces," Trans. Opt. Soc. **23**(3), 141–164 (1922).
8. J. Neauport, C. Ambard, P. Cormont, N. Darbois, J. Destribats, C. Luitot, and O. Rondeau, "Subsurface damage measurement of ground fused silica parts by HF etching techniques," Opt. Express **17**(22), 20448–20456 (2009).
9. J. Neauport, P. Cormont, P. Legros, C. Ambard, and J. Destribats, "Imaging subsurface damage of grinded fused silica optics by confocal fluorescence microscopy," Opt. Express **17**(5), 3543–3554 (2009).
10. E. J. Abbott and F. A. Firestone, "Specifying surface quality: a method based on accurate measurement and comparison," Mech. Eng. **55**, 569–572 (1933).
11. M. Bigerelle and A. Iost, "A numerical method to calculate the Abbott parameters: A wear application," Tribol. Int. **40**(9), 1319–1334 (2007).
12. A. Brient, M. Brissot, T. Rouxel, and J. C. Sangleboeuf, "Influence of grinding parameters on glass workpieces surface finish using response surface methodology," J. Manuf. Sci. Eng. **133**(4), 044501 (2011).
13. AFNOR, "NF EN ISO 13565," in *Geometrical Product Specifications (GPS)–Surface texture: Profile method; Surfaces having stratified functional properties,* (Paris, 1998).

#164889 - $15.00 USD Received 16 Mar 2012; revised 20 Apr 2012; accepted 30 Apr 2012; published 1 Jun 2012

1. Introduction

The 351nm wavelength ns-pulse laser damage of fused silica optics is one of the major limitations of laser facilities such as LMJ (Laser Megajoule) and NIF (National Ignition Facility). Indeed the high fluences, which are subject optics, can cause damage which can grow under subsequent laser shots and thus drastically limit the optics lifetime. Early works have shown that defects present at the interface of fused silica such mechanical subsurface damage [1] can be precursors of laser damage. For example, laser induced damage tests performed on Berkovitch type indentations at the surface of a fused silica sample showed that they could trigger damage at a fluence close to $10J/cm^2$, similar to what is observed on full scale fused silica polished optics [2]. Manufacturing steps of optics, from grinding to polishing, are known to be major contributors to the creation of such mechanical flaws. During grinding step, the diamond grains, present in diamond tools, act as indenters [3] that embrittle locally the material. Based on these considerations the reduction of SSD during the polishing process is of peculiar importance to produce high damage threshold optics.

Knowing the depth of SSD provides essential information to remove these fractures during the various manufacturing stages, and development of fusion class laser facilities has put new focus on this topic. The characterization of SSD is the subject of many studies. The methods used are most often destructive, but some non-destructive methods can also be used. The principle consist generally in achieving a local wear (e.g. ball dimpling [4] or MRF dimpling [5]) or global polishing (e.g. taper polishing or MRF taper) [6] on the workpiece to reveal the micro-cracks whose depth can then be measured by conventional microscopic observation. Such characterizations are generally used to define an empirical relationship between surface roughness (Rt) and depth of defects under surface. Preston [7] reported that the depth of subsurface defects is three times higher than the Peak-to-Valley roughness. Recent studies have shown a good correlation between the maximum SSD depth and the undulation of the surface (4th order moment) [6]. Characterization by chemical method [8] can also be performed, by following, in successive etchings in a HF bath, either the evolution of surface roughness peak to peak *Rt* or the decrease of contaminants. Non-destructive methods (whitelight, tomography, confocal fluorescence microscopy [9] …) can also be performed by probing the interface of the sample without altering the surface of fused silica. However these non-destructive methods only provide access to a localized area and have tends to be significantly inaccurate. Whatever the method, destructive or not, they only give access to the SSD's depth and no information is given on the spatial distribution of the fractures.

In the following study, we investigate the Abbott–Firestone curve [10] or bearing area curve, which describes the surface texture of an object, as an additional indicator to the quality of the glass interface. These Abbott–Firestone parameters give access to the average depth of streaks crisscrossing the surface and to the relative importance of deep fractures existing under the surface.

Analysis of the Abbott–Firestone curves of ground and etched samples provide access not only to the peak to peak value of the SSD but also bring additional information on the distribution of subsurface damage within this peak to peak value. Information on the overall distribution of damage underlying the surface but also on the proportion of damaged areas are obtained. Such information could, for optimized machine parameters, warn us on the need to revive a grinding wheel, alert us on a non-optimal lubrication. Abbott–Firestone curves, as detailed in this paper, have also the advantage to be quite easy to obtain being based on direct use of data provided by roughness measurements when e.g. compared to iterative microscopic observation techniques used to obtain a cumulative crack obscuration as a function of depth into the glass surface [6].

In the first section, the principle of the Abbott–Firestone curve is detailed and illustrated by some examples. Sample preparation and associated characterization are briefly described

#164889 - $15.00 USD Received 16 Mar 2012; revised 20 Apr 2012; accepted 30 Apr 2012; published 1 Jun 2012

in section 3. Results are then presented and discussed in section 4 to then bring our conclusions.

2. Abbott–Firestone curves

The Abbott–Firestone curves are currently used to characterize surface texture. The characterization of friction or also wear of surfaces is improved using the parameters calculated with Abbott–Firestone curves [11] since they give access to both size and proportion of the peaks and valleys of a given surface [12]. Consequently such a characterization method appears to be particularly well suited when ones want to define the proportion of the valleys on a surface such as it's the case for glass surfaces full of subsurface cracks.

Abbott–Firestone parameters are obtained by computing the cumulative probability density function of the surface profile's height by integrating the profile trace. Using the normalization ISO 13565 [13] Abbott–Firestone parameters are defined (Table 1 and Fig. 1) as follows.

Table 1. Abbott–Firestone Parameters

Parameter	Definition
Rk	Roughness core profile
Rpk	Reduced peak height
Rvk	Reduced valley depth
Mr1	Upper material portion
Mr2	Lower material portion

The cumulative probability is divided in 3 areas by means of a tangent at the 40% cumulative probability. The central portion corresponds to the roughness core profile *Rk*. The *Rpk*, *Rvk* parameters are then determined by drawing an horizontal from the intersection of the previous tangent with the vertical axis. The *Rpk* and *Rvk* define areas respectively upper and under the *Rk* area. The *Mr1* and the complementary value of *Mr2* (*100-Mr2*) parameters characterize respectively the percentage of peak and valley, which give information on the peak and valley density of the surface.

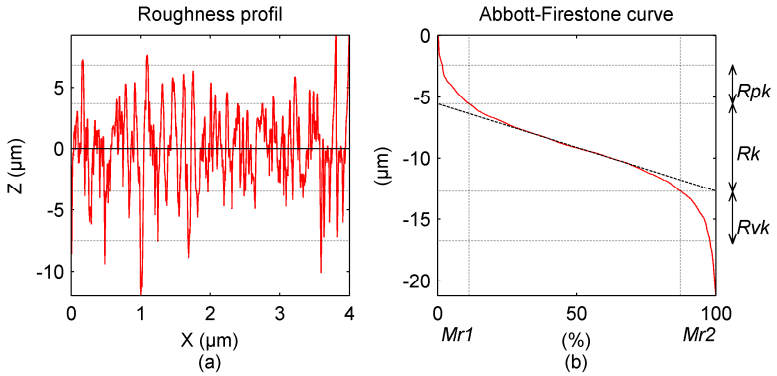

Fig. 1. Abbott–Firestone curve. (a) measured roughness profile trace. (b) the cumulative probability density function of the profile trace analysis allows the computation of Abbott–Firestone parameters.

If *Rk* represents the running surface on which effort are applied, *Rpk* is the reduced peak height that will quickly wear during process and *Rvk* is the reduced valley depth that will tend to subsist at the end of the process and lead to SSD. *Mr1* and *Mr2* are the relative proportion of this peak and valley (if the complementary value of *Mr2* is taking into account) areas in the profile.

#164889 - $15.00 USD Received 16 Mar 2012; revised 20 Apr 2012; accepted 30 Apr 2012; published 1 Jun 2012

An example of an Abbott–Firestone curve obtained on a ground glass surface, without etching, is presented in Fig. 2.

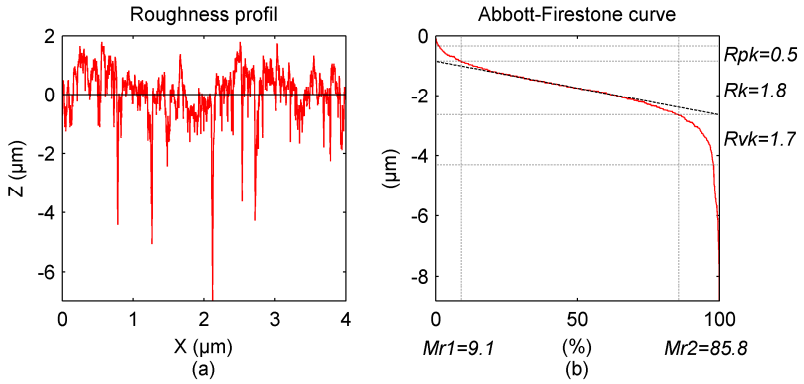

Fig. 2. Typical Abbott–Firestone curve for fused silica sample. (a) measured roughness profile trace. (b) the cumulative probability density function of the profile trace analysis allows the computation of Abbott–Firestone parameters.

For typical surface manufactured with grinding process, the Abbott–Firestone curve (Fig. 2) exhibits an important difference between the *Rpk* and *Rvk* parameters. This difference is characteristic of the surface's topology where the valleys are marked compared to the peaks. The parameter *Mr2* can be interpreted as the density of the valleys of the surface. Indeed, the higher the value of *Mr2* the lower the valleys density will be.

3. Experimentals

3.1 Sample surface preparation

Square-shaped fused silica glass (HOQ from Heraeus) samples (100x100mm^2 x 10mm thick) were used for this study. Roughing was first performed on each sample in order to have the same reference state. Material removal of the first grinding step was then chosen to guarantee a complete removal of residual SSD from the preceding roughing step.

Two sample batches (labeled as Batch A and B) were manufactured on an OPTOTECH SMP500-2C grinder. The samples were grounded using various parameters summarized in Table 2. The samples were ground by blocking the rotation axis of the workpiece table and by translating the grinding wheel in order to be able to only observe the effect of the wheel on the material. Let's outline that this configuration is more damaging for the surface that the usual one for which the two rotations (sample and spindle) are performed simultaneously. Batch A (respectively B), refers to the milling operation using a D126 (respectively intermediate D64) metallic bond diamond wheel. Varying processing conditions were tested with different cutting speed, feed and depth of cut; three values were considered for each parameter. Some samples have been used for both configurations batches A and B.

#164889 - $15.00 USD Received 16 Mar 2012; revised 20 Apr 2012; accepted 30 Apr 2012; published 1 Jun 2012

Table 2. Summary of Operating Conditions for Fused Silica Samples Batches A-B

Batch	Test N°	Wheel	Cutting speed [$m.min^{-1}$]	Feed [$mm.tr^{-1}$]	Depht of cut [mm]
A	1	D126	785	0,015	0,5
	2		785	0,015	1,3
	3		785	0,015	1,5
	4		785	0,04	0,5
	5		785	0,04	1
	6		1167,5	0,0275	0,75
	7		1167,5	0,0275	0,75
	8		1167,5	0,0275	0,75
	9		1167,5	0,0275	0,75
	10		1167,5	0,0275	0,75
	11		1550	0,015	0,5
	12		1550	0,015	1
B	1	D64	785	0,01	0,4
	2		785	0,01	1
	3		785	0,04	0,4
	4		785	0,04	1
	5		785	0,15	1,5
	6		1167,5	0,025	0,75
	7		1167,5	0,025	0,75
	8		1167,5	0,025	0,75
	9		1550	0,01	0,4
	10		1550	0,01	1
	11		1550	0,04	0,4
	12		1550	0,04	1

3.2 Sample characterization

To characterize the precision grinding operation, the surface roughness for each of the ground surfaces was measured by MITUTOYO (SJ-201) contact stylus profilometer, equipped with an inductive probe with 2µm radius and 90° angle. According to the normalized procedure [13], scans of 4mm length were performed, on 16 areas uniformly distributed on the surface of each sample [8]. For each sample, the *Rt* reported in Table 2 is the maximum value obtained on all 16 scans. The roughness Ra and the Abbott–Firestone parameters deduced from the profile measurements are also shown on Table 2. SSD depth was also controlled by means of acid etching; it consists in following the evolution of surface roughness *Rt* during successive hydrofluoric acid (HF) etching. *Rt* is measured after each etching step and the maximal value of *Rt* among the whole set of measurements is equal to the SSD depth as described elsewhere [8]. The surface roughness δ defined by Suratwala [6] is also calculated and reported in Table 3.

#164889 - $15.00 USD Received 16 Mar 2012; revised 20 Apr 2012; accepted 30 Apr 2012; published 1 Jun 2012

Table 3. Roughness, Abbott–Firestone Parameters and SSD Results

Batch	Test N°	Ra [µm]	Rt [µm]	δ [µm]	Rk [µm]	Rpk [µm]	Rvk [µm]	Mr1 [%]	Mr2 [%]	SSDmax [µm]
A	1	0.8	12.9	2.5	1.8	0.3	2.4	5.8	82.7	67.9
	2	1.0	13.4	2.7	2.1	0.5	3.4	7.0	85.2	69.5
	3	1.3	18.0	3.6	2.2	1.1	6.1	8.3	84.7	66.4
	4	1.1	17.3	3.1	2.7	0.6	4.4	6.7	84.7	70.0
	5	1.2	17.0	3.1	3.0	0.5	3.4	8.2	84.6	65.8
	6	1.2	15.5	3.0	1.9	0.3	3.8	6.7	84.3	63.6
	7	0.7	11.4	2.2	1.4	0.3	2.3	6.7	83.1	73.7
	8	1.3	16.2	3.1	2.8	0.5	4.2	6.8	80.7	81.8
	9	1.0	14.4	2.6	2.2	0.4	3.0	6.5	83.9	68.7
	10	0.5	9.6	1.8	1.1	0.2	1.4	6.7	85.0	61.3
	11	1.0	16.6	3.3	1.6	0.4	5.0	7.3	81.7	68.6
	12	1.7	24.5	5.0	2.8	1.0	8.6	8.2	82.2	67.3
B	1	0.8	8.4	1.7	2.0	0.5	2.6	8.5	87.8	38.7
	2	1.2	13.1	2.6	2.9	0.5	3.2	8.4	85.0	36.2
	3	0.9	12.3	2.0	2.2	0.5	2.5	7.3	87.3	47.5
	4	1.0	12.8	2.8	2.0	0.5	4.2	8.3	87.3	44.8
	5	0.7	10.3	1.9	1.3	0.3	2.2	8.1	86.0	38.7
	6	1.6	14.2	2.8	5.0	1.3	4.0	8.4	88.8	41.5
	7	0.8	10.8	2.0	1.8	0.4	2.2	7.2	85.4	33.3
	8	0.9	10.5	2.1	1.8	0.5	2.9	8.3	84.4	42.1
	9	0.7	10.3	1.9	1.3	0.3	2.2	8.1	86.0	38.7
	10	0.7	9.2	1.8	1.8	0.3	2.0	8.1	86.9	36.6
	11	1.2	13.1	2.6	2.9	0.5	3.2	8.4	85.0	36.2
	12	0.8	9.0	1.7	2.0	0.4	2.3	7.4	85.2	32.6

4. Results and discussions

Using the results presented in previous section, some indicators based on ratios between the SSD depth and the roughness parameters can be analyzed (Table 4).

Table 4. Indicators Definition

Indicator		Definition
k_{Rt}	=	SSD/Rt
k_{δ}	=	SSD/δ
k_{Rk}	=	SSD/Rk
k_{Rpk}	=	SSD/Rpk
k_{Rvk}	=	SSD/Rvk
k_{Mr1}	=	SSD/Mr1
k_{Mr2}	=	SSD/Mr2

The evolutions of parameters proposed in Table 4 are presented in the curves hereafter. Let's outline that following figures will be presented with the test number in abscissa. Points are plotted in the same order than presented on Table 2. Such a representation is done to compare the relative evolution of the different indicators for the different diamond wheels (batches A and B) and cutting conditions.

The results of k_{Rt} and k_{δ} indicators presented on the Fig. 3 appear to be quite scattered and far from the results of the Suratwala who established values of $k_{Rt} = 9.1$ and $k_{\delta} = 49$ [6]. Such behavior has already been demonstrated in other studies [8]. For the chosen configuration of machining and for two different types of wheel, it can be concluded that these k_{Rt} and k_{δ} indicators are dependent on the process, the type of tool, the kinematic conditions …

#164889 - $15.00 USD Received 16 Mar 2012; revised 20 Apr 2012; accepted 30 Apr 2012; published 1 Jun 2012

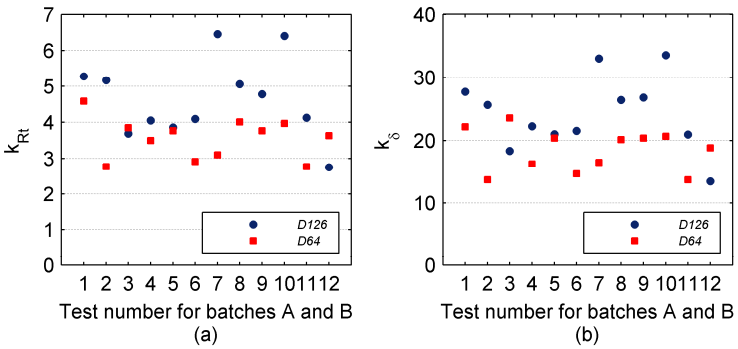

Fig. 3. *Rt* (a) and δ (b) bibliographic indicators evolution [6].

The results of k_{Rk}, k_{Rpk} and k_{Rvk} indicators are presented on the Fig. 4. The results of these indicators are as scattered as previous indicators (Fig. 3). It can be concluded that these indicators are also dependent on cutting conditions and wheel type.

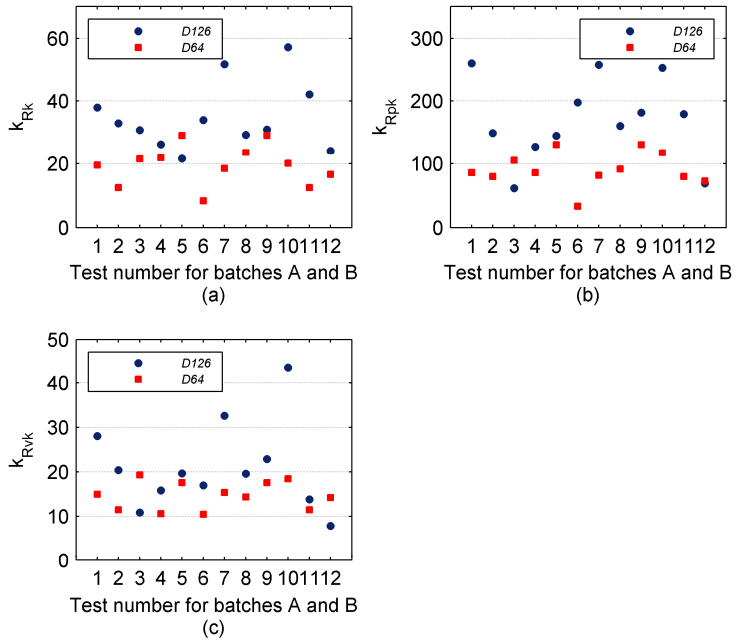

Fig. 4. *Rk* (a), *Rpk* (b)and *Rvk* (c) Abbott–Firestone indicators evolution.

In the Fig. 5, the parameters involving *Mr1* and *Mr2*, respectively, show that a relationship between peaks and valleys densities and the depth of SSD can be expressed. The *Mr1* and *Mr2* parameters appear to be relatively independent of kinematic conditions. However, the results show a strong dependence on the size and density (D126 or D64) of the wheel.

#164889 - $15.00 USD Received 16 Mar 2012; revised 20 Apr 2012; accepted 30 Apr 2012; published 1 Jun 2012

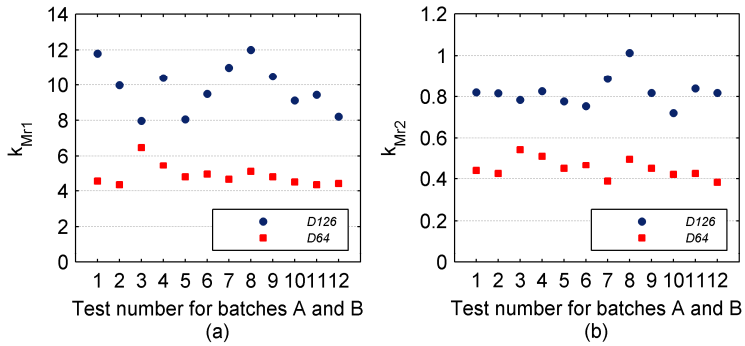

Fig. 5. *Mr1* (a) and *Mr2* (b) Abbott–Firestone indicators evolution.

Considering typical roughness profiles such as obtained on a diamond ground glass surfaces (Fig. 2), the more pertinent parameters characterizing both damage and topology of the such surfaces are both the depth of SSD and the *Mr2* Abbott–Firestone parameter.

It is also observed (Fig. 6) that whatever the cutting conditions (spindle speed, feed rate), the wheel with the smaller particle size generates the lowest SSD's depth and upper valleys density. In our experimental study the influence of the particle density, for a given particle size, has not been studied. However, this parameter could affect the density of SSD; but this remains to be confirmed by additional tests.

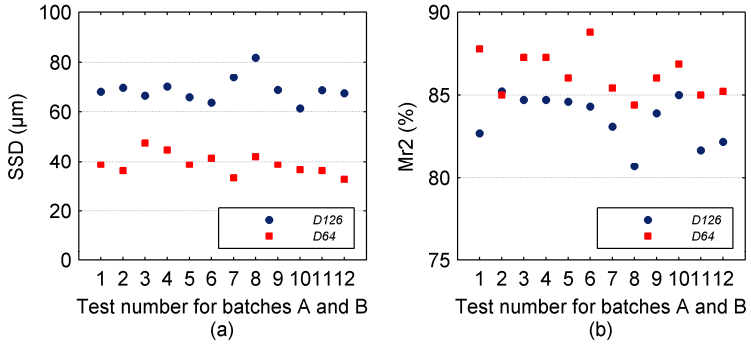

Fig. 6. *SSD* (a) and *Mr2* (b) Abbott–Firestone parameter evolution.

Thus, the tests conducted in this study allow one hand to show that the indicators currently used are too dependent on experimental conditions and also to provide opportunities for the development of new indicators more relevant through the use of Abbott–Firestone parameters.

5. Conclusion and prospects

Characterization of the SSD is a crucial step to determine optimal process parameters to manufacture laser optics. We investigated the relative evolution of various surface profile indicators on a variety of diamond ground surfaces manufactured with different cutting conditions and diamond wheels. It is evidenced that the parameters usually used to estimate SSD from a roughness profile such as roughness peak to peak *Rt* or 4th order moment δ are highly dependent on manufacturing conditions. On the contrary, k_{Mr2}, based on Abbott–Firestone curves seems to be more representative of SSD since it appears to stay constant when changing manufacturing parameters. We also evidenced a significant influence of the grinding parameters (grain size, grain density). This behavior shall be further analyzed by additional experiments.

#164889 - $15.00 USD Received 16 Mar 2012; revised 20 Apr 2012; accepted 30 Apr 2012; published 1 Jun 2012

Acknowledgments

This work is supported by the Conseil Régional d'Aquitaine and is performed in the framework of the EFESO project.

#164889 - $15.00 USD Received 16 Mar 2012; revised 20 Apr 2012; accepted 30 Apr 2012; published 1 Jun 2012